t-SNARE dephosphorylation promotes SNARE assembly and exocytosis in yeast

Michael Marash and Jeffrey E.Gerst[1]

Department of Molecular Genetics, Weizmann Institute of Science, Rehovot 76100, Israel

[1]Corresponding author
e-mail: jeffrey.gerst@weizmann.ac.il

The role of protein phosphorylation in secretion is not well understood. Here we show that yeast lacking the Snc1,2 v-SNAREs, or bearing a temperature-sensitive mutation in the Sso2 t-SNARE, are rescued at restrictive conditions by the addition of ceramide precursors and analogs to the growth medium. Rescue results from dephosphorylation of the Sso t-SNAREs by a ceramide-activated type 2A protein phosphatase (Sit4) involved in cell cycle control. Sso t-SNARE dephosphorylation correlated with its assembly into complexes with the Sec9 t-SNARE, both *in vitro* and *in vivo*, and with an increase in protein trafficking and secretion in cells. SNARE complexes isolated under these conditions contained only Sso and Sec9, suggesting that a t–t-SNARE fusion complex is sufficient to confer exocytosis. Mutation of a single PKA site (Ser79 to Ala79) in Sso1 resulted in a decrease in phosphorylation and was sufficient to confer growth to *snc* cells at restrictive conditions. Thus, modulation of t-SNARE phosphorylation regulates SNARE complex assembly and membrane fusion *in vivo*.

Keywords: protein phosphorylation/Sec9/SNARE/Snc/Sso

Introduction

Intracellular protein trafficking and membrane fusion is mediated, in part, by three conserved families of membrane-associated proteins, known as SNAREs (Ferro-Novick and Jahn, 1994; Rothman and Warren, 1994). SNAREs on the vesicular/donor membranes (v-SNAREs) interact *in trans* with cognate partners present on target membranes (t-SNAREs) to assemble into a complex that brings the bilayers into close proximity and is energetically favorable for fusion (Rothman and Warren, 1994). SNAREs, by themselves, appear to contain the information necessary and sufficient for membrane fusion to occur *in vitro* (Weber *et al*., 1998; McNew *et al*., 2000).

The synaptic SNARE complex consists of four α-helices arrayed in parallel to form a four-helix bundle, with three helices donated by the t-SNAREs and one by the v-SNARE (Sutton *et al*., 1998). Members of the three SNARE families (e.g. the syntaxin, SNAP-25 and synaptobrevin/VAMP families) are also typed according to the charged amino acid [i.e. glutamine (Q) or arginine (R)] present in the ionic layer of the bundle (Fasshauer

et al., 1998). According to this classification, the SNARE complex consists of two Q-SNAREs and one R-SNARE.

SNAREs act at all levels of the yeast secretory pathway, including anterograde and retrograde transport steps (Ferro-Novick and Jahn, 1994; Pelham, 1997; Gotte and Fischer von Mollard, 1998). Disruptions in SNARE-encoding genes that confer transport from the endoplasmic reticulum (ER) to the Golgi, and from the Golgi to the plasma membrane (PM), result in severe trafficking defects or lethality. For example, deletions in the *SNC1,2* genes, which confer Golgi-to-PM anterograde and retrograde transport, result in conditional lethality (Gerst *et al*., 1992; Protopopov *et al*., 1993; Gurunathan *et al*., 2000). Cells lacking the *SNC* genes are deficient in the docking and fusion of secretory vesicles (SVs), resulting in their accumulation and a loss in secretion competence (Protopopov *et al*., 1993). Despite this, *snc* cells grow slowly on synthetic medium at ≤30°C, suggesting that some SV fusion occurs in the absence of exocytic v-SNAREs.

Recently, we identified two genes that, when inactivated, restored growth and protein trafficking in *snc* yeast. Mutations in either *VBM1* or *-2* led to the re-coupled transport of at least one of two SV populations controlled by the Snc v-SNAREs (David *et al*., 1998). Thus, the *VBM* gene products act in an inhibitory fashion upon SV docking and fusion. Interestingly, *VBM1,2* are identical to *ELO2,3*, whose products confer fatty acid elongation to yield the long chain (C_{26}) fatty acids (LCFAs) required for ceramide and sphingolipid (SL) synthesis (Oh *et al*., 1997). Single gene knockouts led to a decrease in both SL levels and composition in wild-type (WT) and *snc* yeast (Oh *et al*., 1997; David *et al*., 1998), as well as an increase in phytosphingosine (PHS), a ceramide precursor (Oh *et al*., 1997). We hypothesized that either phenomenon might be sufficient to re-couple SV trafficking (David *et al*., 1998).

Here, we show that treatment of *snc* cells with ceramide precursors or analogs ameliorates growth and confers a v-SNARE bypass (VBM) effect. In both *snc vbm* and ceramide/PHS-treated *snc* cells, Sso t-SNAREs are dephosphorylated and form complexes with the Sec9 t-SNARE. Dephosphorylation is mediated by a known ceramide-activated protein phosphatase (CAPP), Sit4 (Nickels and Broach, 1996). Correspondingly, mutation of a protein kinase A (PKA) site (Ser79 to Ala79) in Sso1 was sufficient to rescue *snc* cells in the absence of ceramide. Finally, recombinant Sso1 phosphorylated *in vitro* by Tpk1 was deficient in its ability to assemble into complexes with Sec9.

Three significant findings were surmised. First, t-SNARE phosphorylation by the PKA pathway inhibits SNARE assembly and subsequent membrane fusion in yeast. Secondly, a sphingoid base/ceramide-regulated
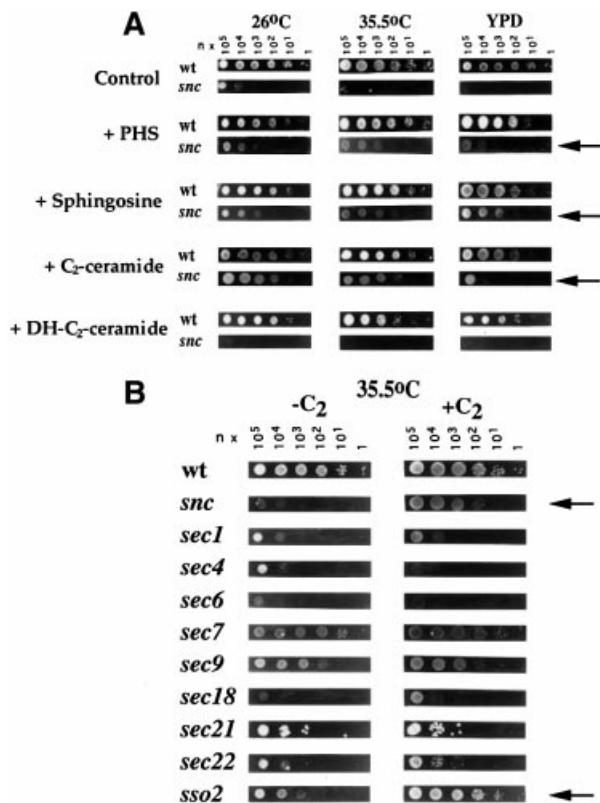
Fig. 1. Exogenous addition of sphingoid bases and a ceramide analog rescues *snc* and *sso2-1* cells. (**A**) *snc* cells grown on glucose-containing medium (24 h) were diluted serially (*n*, number of cells = 19) and placed onto rich medium (YPD) or SC medium (26 and 37°C), either with or without added sphingoid bases or ceramide analogs. Bases included PHS (25 µM), sphingosine (10 µM) and sphinganine (10 µM) (not shown). Analogs included C_2-ceramide and DHC_2-ceramide (10 µM). (**B**) Early (*sec18-1*, *21-1* and *22-1*), middle (*sec7-1*) and late (*sec1-1*, *4-8*, *6-4*, *9-4* and *sso1Δ sso2-1*) secretory mutants were grown to log phase at 26°C prior to dilution (*n* = 3) and plating onto medium with or without C_2-ceramide. Cells were grown for 36 h.

signaling pathway restores exocytosis by dephosphorylating the t-SNAREs. Thirdly, t-SNAREs confer SV docking and fusion in the absence of their v-SNARE partners, as proposed by David *et al*. (1998).

Results

Exogenous addition of ceramide precursors or analogs rescues snc cells and confers a v-SNARE bypass effect

Yeast lacking the Snc v-SNAREs accumulate SVs, are deficient in protein secretion and grow at ≤30°C only (Protopopov *et al*., 1993; David *et al*., 1998). *VBM1/ELO3* and *VBM2/ELO2* were identified as genes that, when inactivated, confer v-SNARE-independent exocytosis and normal growth to *snc* cells (David *et al*., 1998). Nevertheless, secretion from these cells is fully dependent upon the exocytic t-SNAREs, Sso1,2. Interestingly, the *VBM* genes encode ER-localized proteins that confer LCFA elongation and SL synthesis (Oh *et al*., 1997; David *et al*., 1998). Thus, the VBM phenotype arises due to a decrease in SL levels or an increase in SL precursors, both of which occur in *vbm/elo* cells (Oh *et al*., 1997; David *et al*., 1998).

To distinguish between these possibilities, we added phytosphingosine (PHS), a ceramide precursor that accumulates in *elo/vbm* cells (Oh *et al*., 1997), to *snc* yeast and examined their ability to grow at restrictive conditions. We employed this method as there is no precise way to modulate SL levels *in vivo* and because the overexpression of genes involved in SL synthesis (i.e. *LCB1*, *SUR2*, *AUR1*, *SCS7*, *CSG1* and *CSG2*, etc.) had no effect upon the growth of *snc* cells (not shown).

We found that PHS (25 µM) or sphingosine (10 µM) addition conferred growth on amino acid-rich medium (YPD) and at 35.5°C on synthetic medium (Figure 1A). The concentrations used were those that gave maximal effect (not shown). Growth in the presence of these additions was not as robust as that of *snc* yeast mutated in either *VBM/ELO* gene, which closely approximates that of WT cells (David *et al*., 1998 and data not shown). An inactive form of sphingosine, dihydro-D-*erythro*-sphingosine (sphinganine) (10 µM), had no effect whatsoever (not shown).

As PHS is metabolized to SL via ceramide synthase (Lester and Dickson, 1993), we tested whether a cell-permeable ceramide analog, C_2-ceramide (*N*-acetyl-D-*erythro*-sphingosine), had similar effects. This analog stimulates the activity of type 2A phosphatases in yeast (Fishbein *et al*., 1993; Nickels and Broach, 1996) and has anti-proliferative properties in some strains. We found that C_2-ceramide (10 µM) conferred an effect identical to PHS or sphingosine upon *snc* cells, and restored partial growth on YPD and at 35.5°C (Figure 1A and B). This was observed at concentrations as low as 1 µM (not shown). In contrast, the addition of C_2-ceramide to WT cells had only mild deleterious effects upon growth, while the addition of dihydro-C_2-ceramide (DHC_2-ceramide), an inactive form, had none (Figure 1A). Metabolism of DHC_2-ceramide to C_2-ceramide (via *SUR2*) is unlikely to occur in quantity, due to the slow metabolism of *snc* cells (Protopopov *et al*., 1993; David *et al*., 1998).

Addition of C₂-ceramide rescues cells bearing a mutant sso2-1 allele

Next we determined whether the temperature sensitivity of secretion (*sec*) mutants is affected by ceramide addition. We examined the growth of cells bearing temperature-sensitive (*ts*) mutations in the *SEC1*, *4*, *6*, *7*, *9*, *18*, *21*, *22* or *SSO2* genes under restrictive conditions (Figure 1B). We found that cells bearing a *ts* mutation in *SSO2* (*sso1Δ sso2-1* cells) were rescued at 35.5°C by the addition of C_2-ceramide. In contrast, no other *sec* mutant was strongly affected, although the growth of cells that express a mutant Sec22 v-SNARE was mildly improved. Given that *snc* and *snc vbm* cells are dependent upon the *SSO* gene products for viability (David *et al*., 1998) and that C_2-ceramide treatment ameliorates *ts* defects in *sso2-1* cells, it appears that the target of ceramide regulation might be the Sso t-SNAREs.

Addition of C₂-ceramide partially restores trafficking in snc cells

As *snc* null cells grow well in the presence of C_2-ceramide, we examined their intracellular morphology and ability to synthesize and traffick proteins. *snc* yeast accumulate SVs (Protopopov *et al*., 1993); however, thin sections of *snc*
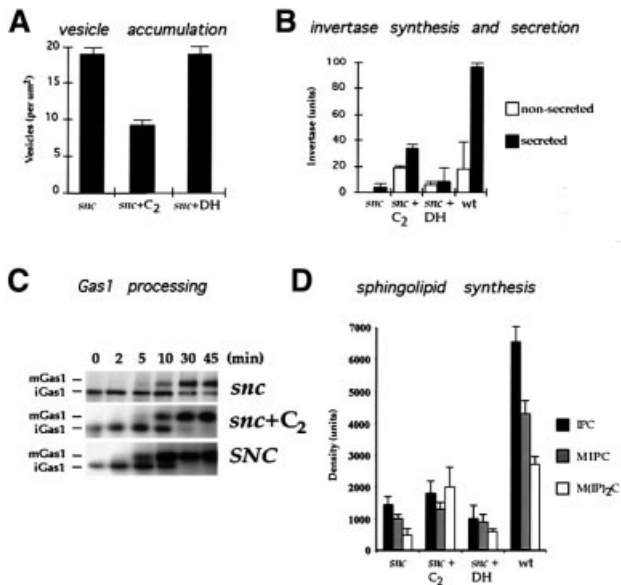
Fig. 2. C_2-ceramide partially restores trafficking functions in *snc* cells. (**A**) Vesicle accumulation in treated and untreated *snc* cells. *snc* cells were grown to log phase with or without added C_2-ceramide (C_2) or the inactive DHC_2-ceramide (DH) (10 µM). Cells were sectioned and the number of vesicles per µm^2 determined. (**B**) Invertase secretion from treated and untreated *snc* cells. *snc* cells were grown as in (A), prior to de-repression (2 h) in low glucose medium to induce invertase expression. WT yeast were used as control. Secreted and non-secreted activities were determined. (**C**) Gas1 processing in treated and untreated *snc* cells. *snc* cells were grown as in (A), prior to pulse–chase labeling with [^{35}S]methionine. Gas1 protein was immunoprecipitated, electrophoresed and autoradiographed. *SNC* indicates *snc* cells expressing *SNC1* constitutively, as control. Chase is given in minutes. (**D**) SL synthesis in treated and untreated *snc* cells. *snc* cells were grown as in (A), prior to labeling with [^{3}H]*myo*-inositol, SL extraction and thin-layer chromatography. Histograms show the values obtained from autoradiography. *IPC*, inositol-phosphorylceramide; *MIPC*, mannosyl-IPC; *M(IP)$_2$C*, mannosyl(inositol-phosphoryl)$_2$ceramide.

cells grown in the presence of C_2-ceramide revealed a significant decrease in their number (Figure 2A). Control *snc* cells had 18 ± 1 vesicles/µm^2 (*n* = no. of cells examined = 30), whereas cells grown in the presence of C_2-ceramide had only 8 ± 0.6 vesicles/µm^2 (*n* = 30). In contrast, *snc* cells grown in the presence of DHC_2-ceramide showed no change in the number of vesicles (18 ± 1.3 vesicles/µm^2, *n* = 30). We noted that the intracellular localization of SVs in treated cells was unchanged with respect to untreated cells, being present in both mother and bud (not shown). Interestingly, the reduction in the number of SVs per unit area in treated cells corresponded well with that observed for *snc vbm* cells (David *et al.*, 1998). Thus, C_2-ceramide treatment approximates mutations in the *VBM/ELO* genes in many respects.

snc cells treated with C_2-ceramide show enhanced growth capabilities that correspond with a reduction in the number of untrafficked SVs. This is expected to enhance protein trafficking as well as secretion. We examined the synthesis and secretion of invertase, which is severely reduced in *snc* cells (Protopopov *et al.*, 1993; Gerst, 1997). We found that invertase synthesis (total secreted and non-secreted activities) was elevated 12-fold in *snc* cells

treated with C_2-ceramide, while the amount secreted was 8-fold higher (Figure 2B). In contrast, *snc* cells synthesized and secreted a tiny, though proportionally larger, amount of enzyme. This varied between experiments; thus, it is unlikely that invertase trafficking is faster in untreated cells. Finally, WT cells were found to synthesize and secrete 2- to 3-fold more enzyme than ceramide-treated cells. Thus, ceramide treatment partially restores invertase synthesis and secretion in *snc* cells, while its inactive analog (DHC_2-ceramide) had little effect (Figure 2B).

The intracellular processing of Gas1, a GPI-anchored protein, is slowed in *snc* cells due to the low rates of protein and LCFA/SL synthesis (David *et al.*, 1998). To test whether C_2-ceramide restores Gas1 processing, we performed pulse–chase analysis using [^{35}S]methionine in treated and untreated *snc* cells. We found that Gas1 processing was similar to that of WT cells after treatment (Figure 2C). In contrast, untreated cells still had immature Gas1 present after 45 min of chase.

As mutations in the *VBM/ELO* genes reduce the level and content of SLs (Oh *et al.*, 1997; David *et al.*, 1998), we determined whether C_2-ceramide treatment has similar effects upon *snc* cells. *snc* cells normally synthesize less SLs, but all three types are reduced equally (David *et al.*, 1998). This reduction in synthesis results from a slow metabolic rate and not from defects in lipid processing. We examined SL synthesis in *snc* cells treated with C_2-ceramide by metabolic labeling with [^{3}H]*myo*-inositol (Figure 2D). We found an increase in SL synthesis and, in particular, the Golgi-modified SL mannose (inositolphos-phoryl)$_2$-ceramide ($M(IP)_2C$) was elevated 3-fold to reach WT levels. This contrasts with *snc vbm* cells, in which large reductions in SL levels, particularly those of $M(IP)_2C$, were observed (David *et al.*, 1998). Thus, rescue of *snc* phenotype by ceramide is not likely to occur via changes in intracellular SL content.

These results show that ceramide treatment improves protein and lipid biosynthesis, enhances the trafficking of SVs and restores intracellular protein trafficking in *snc* yeast.

Sso t-SNAREs are dephosphorylated upon treatment with C_2-ceramide or by *vbm* mutation

As ceramide treatment rescues *snc* and *sso2-1* cells at restrictive temperatures and is known to activate CAPP, we examined whether the Sso t-SNAREs are substrates for this phosphatase. We labeled WT and *snc* yeast with [^{32}P]orthophosphate and isolated Sso proteins by immuno-precipitation (IP) using affinity-purified anti-Sso anti-bodies (abs) (Figure 3A). Between 8.4 and 10.2% of total cellular Sso was immunoprecipitated from the extracts. We found that Sso was weakly labeled in C_2-ceramide-treated and untreated WT cells (Figure 3A). In contrast, untreated *snc* cells had 8-fold higher levels of Sso phosphorylation, but this could be abolished upon treat-ment with C_2-ceramide (Figure 3A and B). This demon-strates that Sso proteins are phosphorylated *in vivo* and dephosphorylated in response to ceramide treatment.

Since the mechanism by which inactivating mutations in the *VBM* genes rescue *snc* cells could be similar, we examined Sso phosphorylation in *snc* and WT cells bearing *vbm* mutations by metabolic labeling and IP
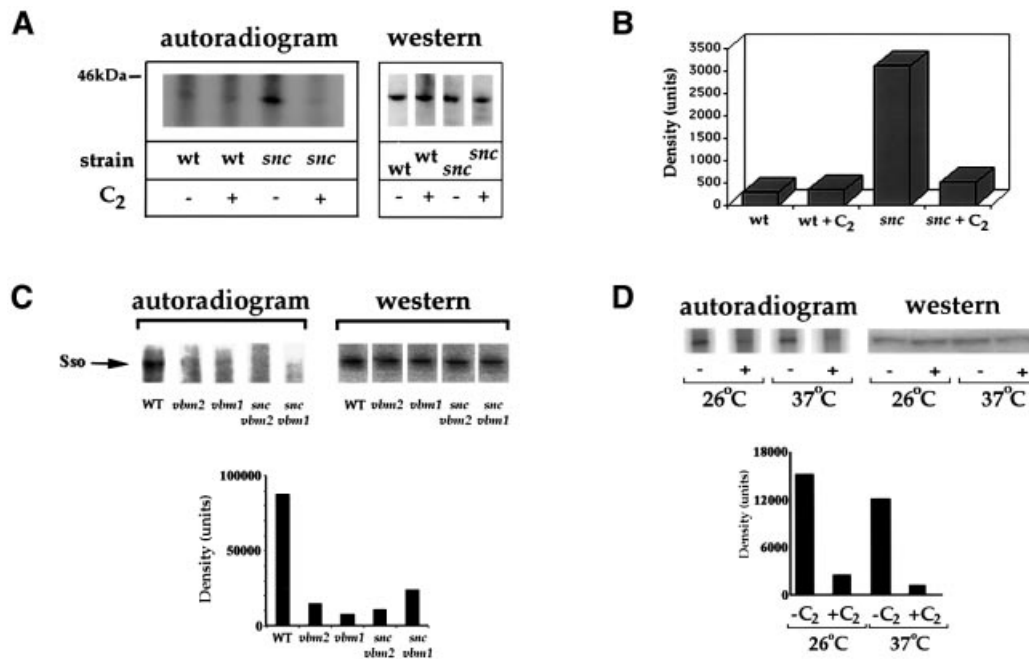
Fig. 3. Sso t-SNAREs undergo dephosphorylation upon treatment with C_2-ceramide or *vbm* mutation. (**A**) Sso is dephosphorylated upon treatment with C_2-ceramide. *snc* or WT cells were grown to log phase in SC with ($+C_2$) or without ($-C_2$) C_2-ceramide (10 μM). Cells were labeled with [^{32}P]orthophosphate. Sso protein was immunoprecipitated using anti-Sso abs and detected on blots (western) with anti-Sso abs, or in gels by exposure (autoradiogram). (**B**) Histogram of the radiography data in (A), after normalization for Sso expression. Density is in arbitrary units. (**C**) Sso is dephosphorylated upon *vbm* mutation. WT, *vbm1*, *vbm2*, *snc vbm1* and *snc vbm2* cells were labeled and processed, as in (A). A histogram of the radiography data, normalized for protein expression, is shown below. (**D**) Mutant Sso2 is dephosphorylated in response to ceramide treatment. *sso2-1* cells were labeled as in (A). Sso2-1 was immunoprecipitated and detected on blots (western) using anti-Sso abs or in gels by autoradiography (autoradiogram). A histogram of the radiography data from (D), after normalization for Sso2-1 expression, is shown below.

(12.1–13.2% of total Sso immunoprecipitated). We found >80% less label was incorporated into Sso in *snc* or WT cells bearing *vbm* mutations (Figure 3C). Thus, *VBM* gene inactivation also induces Sso dephosphorylation. This implies that t-SNARE dephosphorylation is central to the mechanism of rescue operative in both *snc vbm* and ceramide-treated *snc* cells.

As ceramide treatment rescued *sso2-1* cells at restrictive temperatures, next we examined whether the dephosphorylation of mutant Sso2 is apparent (Figure 3D). Metabolic labeling of *sso2-1* cells and IP of Sso2-1 (between 11.9 and 13.2% of total) revealed that the protein became dephosphorylated by ~80% upon ceramide treatment at either 26 or 37°C (Figure 3D). Thus, ceramide-mediated t-SNARE dephosphorylation occurs in cells having their full complement of exocytic v-SNAREs and is not an artifact of the loss of Snc expression.

Sso dephosphorylation promotes t-SNARE assembly in snc cells

To examine the consequence of Sso dephosphorylation *in vivo*, we measured the amount of Sso complexed with Sec9 (a yeast SNAP-25 homolog) in C_2-ceramide treated and untreated cells (Figure 4A and B). The amount of Sso–Sec9 in association should reflect the amount of vesicle fusion that had occurred (i.e. *trans* complexes formed) prior to Sec18-mediated dissociation of the complex (Carr *et al.*, 1999). We immunoprecipitated SNAREs from both treated and untreated *snc* cells using affinity-purified anti-Sec9 (C-terminus, Sec9$^{402–651}$) or

anti-Sso abs. The immunoprecipitated SNAREs were resolved on gels and detected by quantitative western analysis. We also measured the amount of the partner t-SNAREs that co-immunoprecipitated with these abs, i.e. the amount of Sec9 that co-immunoprecipitated with anti-Sso abs and vice versa. This allowed us to measure the amounts (in moles) of t-SNAREs present in complexes. We made several adjustments to improve detection and accuracy. First, total cell lysate (TCL) samples were normalized (for the amount of either t-SNARE) between treated and untreated cells to account for variations in SNARE expression or recovery. Secondly, IP of the SNAREs was performed using a set concentration of abs to precipitate between 10 and 13% of each SNARE present in the TCL. Thirdly, to measure the molar equivalents of the t-SNAREs present in the TCLs, supernatants and immunoprecipitates, we used purified recombinant Sso1$^{1–265}$ and Sec9$^{402–651}$ as standards for the SNAREs in western blots (Figures 4 and 5). Known quantities of recombinant SNAREs were electrophoresed and detected in parallel to the other samples. Detection was performed quantitatively using the same concentrations of purified anti-Sec9 or -Sso abs.

Upon ceramide treatment we found no change in the levels of SNARE expression, but did find that the amount of Sec9 and Sso present in complexes was elevated 3-fold (average = 3.5 ± 0.6-fold, $n = 5$ experiments) in C_2-ceramide-treated *snc* cells *vis-à-vis* untreated cells (Figure 4A and B). In the experiment shown in Figure 4A, 0.4 E-7 and 1.1 E-7 mol (0.7 and 2.4%) of
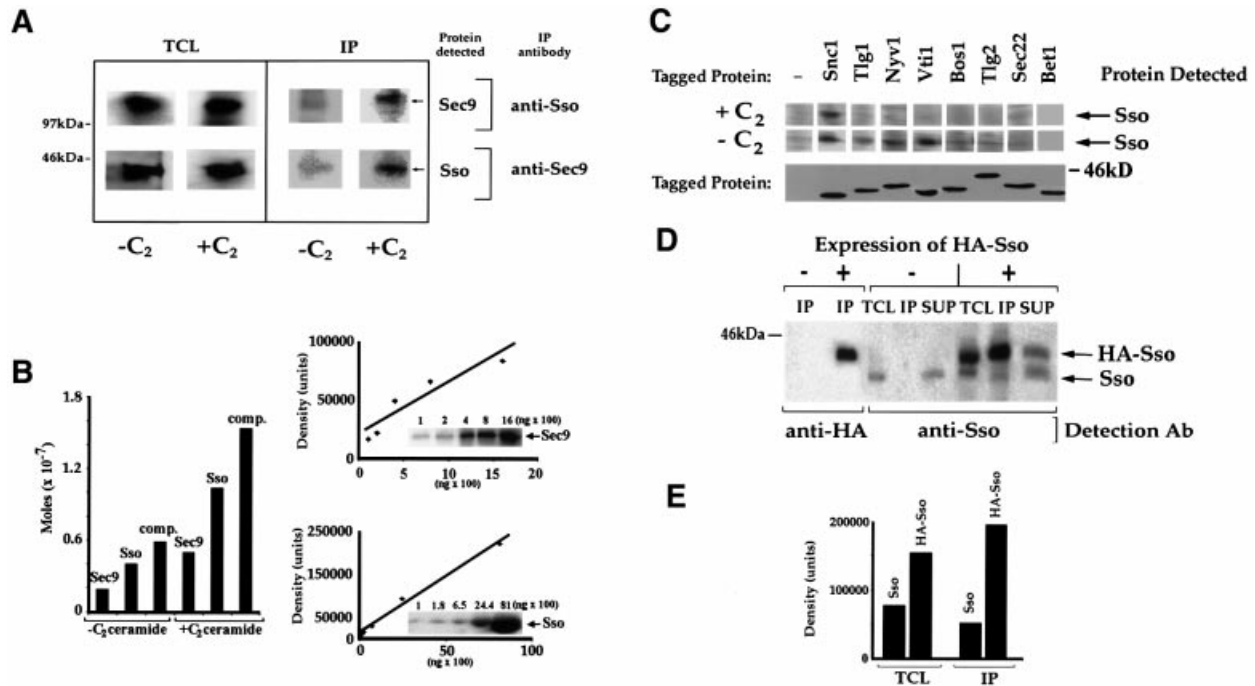
Fig. 4. Sso dephosphorylation promotes t-SNARE assembly in *snc* cells. (**A**) C_2-ceramide promotes Sso–Sec9 complex assembly. *snc* cells were grown to log phase with (+C_2) or without (–C_2) C_2-ceramide (10 µM). Sso and Sec9 were immunoprecipitated and detected quantitatively in reciprocal fashion, using purified anti-Sec9 or anti-Sso abs. TCL, total cell lysate (100 µg protein/lane). (**B**) Left panel: histogram of the IP data shown in (A), after normalization. Density is in arbitrary units. Right panel: standard curves used in the determination of Sso and Sec9 in complexes. Recombinant GST–Sso1[1–265] and GST–Sec9[402–651] proteins were electrophoresed and detected in parallel to the IP/TCL samples. (**C**) C_2-ceramide promotes Sso disassembly from non-specific SNARE interactions. *snc* cells expressing epitope-tagged v- and t-SNAREs (e.g. HA-Snc1, HA-Tlg1, HA-Tlg2, HA-Vti, HA-Bos1, myc-Nyv1, myc-Sec22 and myc-Bet1) from plasmids were grown in medium with (+C_2) or without (–C_2) C_2-ceramide. Top panel: tagged proteins were immunoprecipitated using anti-tag abs and Sso was detected quantitatively in the precipitates using anti-Sso abs. Bottom panel: expression of tagged SNAREs was verified using anti-tag abs. (**D**) Sso proteins co-precipitate. *snc* cells expressing HA-Sso1 were grown to log phase with added ceramide. HA-Sso1 was immunoprecipitated from extracts with anti-HA abs, while quantitative detection of tagged and native Sso was performed on blots using anti-HA and anti-Sso abs, respectively. TCL, total cell lysate (75 µg protein/lane); IP, immuno-precipitate; SUP, the supernatant retained after IP (5% of total SUP loaded). (**E**) Histogram of the data in (D) showing the amounts of tagged/native Sso in the TCLs and IPs, before normalization. Density is in arbitrary units.

Sso co-immunoprecipitated with anti-Sec9 abs, while 0.2 E-7 and 0.5 E-7 mol (0.5 and 1.3%) of Sec9 co-immunoprecipitated with anti-Sso abs, from extracts derived from untreated and treated cells, respectively. Similar results were also obtained using PHS instead of ceramide (not shown). Thus, dephosphorylation correlates with the enhanced assembly of Sso and Sec9 into t–t-SNARE complexes.

Ceramide treatment increases SNARE complex formation in sso2-1 cells

Next, we determined the amount of Sso2-1 present in complexes with Sec9 in *sso2-1* cells after treatment with ceramide. We found that the amount of Sso2-1 that co-precipitated with anti-Sec9 abs increased, on average, by 2.2 ± 0.4-fold ($n = 3$ experiments) in treated cells (not shown). Thus, ceramide treatment promotes SNARE assembly even in the presence of the exocytic v-SNAREs.

Some phospho-Sso is present in SNARE complexes

We next determined whether phosphorylated Sso is present in the Sso–Sec9 SNARE complex by labeling *snc* cells with [^{32}P]orthophosphate and immunoprecipitating Sso. Although we did not know the amount of

unlabeled phosphate present in Sso, we postulated that the levels of incorporated label might be modulated by ceramide treatment. This would allow us to estimate the amount of phosphate that is sensitive to CAPP activity *in vivo*. We found that the molar ratio of incorporated labeled phosphate to total Sso protein (as immunoprecipitated and quantitated using anti-Sso abs) declined by 55% after ceramide treatment (from 1.15 E-9:1 to 0.62 E-9:1). Similarly, the molar ratio of labeled phosphate to Sso protein found in a complex with Sec9 (as immunoprecipitated by anti-Sec9 abs) declined by 65% after treatment (from 8.2 E-10:1 to 3.0 E-10:1). Molar equivalents of label and Sso protein were determined using carrier-free [^{32}P]phosphate and purified Sso1[1–265] as standards for autoradiography and western analysis, respectively. Thus, some phosphorylated Sso is present in the SNARE complex *in vivo*, but these phosphate groups are probably unrelated to CAPP activity and SNARE assembly (see Figure 5B and C).

Non-specific v- and t-SNARE interactions with Sso are eliminated upon ceramide treatment

Another v-SNARE could be operative in *snc* or *snc vbm* cells, although genetic studies provide no evidence for this (David *et al*., 1998). In fact, no other gene when
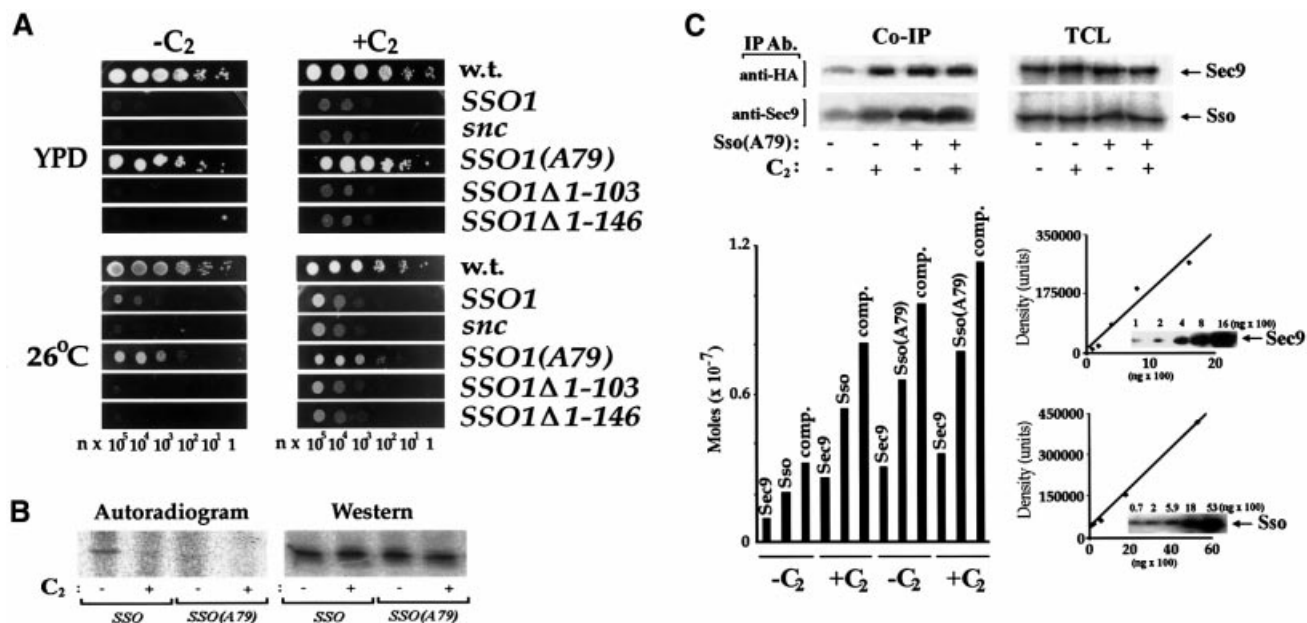
Fig. 5. Mutation of Ser79 in Sso1 rescues *snc* cells in the absence of ceramide. (**A**) Expression of Sso[Ala79] rescues *snc* cells. *snc* cells transformed with plasmids expressing HA-tagged Sso1, Sso[Ala79], Sso1[Δ1–103], Sso1[Δ1–146] or a control plasmid (*snc*) were grown on galactose-containing medium, prior to transfer to glucose medium (24 h) to deplete Snc1. Cells were diluted (*n* = 2) onto SC (26°C) and rich medium (YPD), with (+C_2) or without (–C_2) C_2-ceramide, and grown (24 h). (**B**) Sso1[Ala79] is under-phosphorylated. *snc* cells expressing HA-Sso1 or HA-Sso1[Ala79] from plasmids were grown to log phase in medium with (+) or without (–) C_2-ceramide (10 µM). Cells were labeled with [^{32}P]orthophosphate (as in Figure 3A), Sso protein was immunoprecipitated and detected on blots with anti-HA abs (western) or in gels by exposure (autoradiogram). (**C**) Sso1[Ala79] complexes with Sec9 in the absence of ceramide. *snc* cells expressing HA-Sso1 or HA-Sso1[Ala79] were grown with (+) or without (–) C_2-ceramide (10 µM). HA-Sso and Sec9 proteins were immunoprecipitated and detected quantitatively in reciprocal fashion. Lower left panel: histogram of the amounts of HA-Sso proteins and Sec9 precipitated. Complex indicates the amount of Sso protein (Sso or Sso1[Ala79]) complexed with Sec9. Lower right panel: standard curves for the determination of Sso and Sec9 present in the TCL or IP lanes.

overexpressed can fully rescue *snc* cells, except for *SNC1* or *2*. Nevertheless, we overexpressed other v- and t-SNAREs in *snc* cells and examined their ability to: (i) facilitate rescue upon ceramide treatment and (ii) associate with Sso. Over-production of tagged Bet1, Bos1 and Sec22 (ER–Golgi v-SNAREs), Tlg1 (*trans*-Golgi t-SNARE), Vti1 and Nyv1 [prevacuolar compartment (PVC) and vacuolar v-SNAREs], Pep12 and Tlg2 (PVC and endosomal t-SNAREs) did not enhance the growth of *snc* cells, even in the presence of ceramide (not shown). As SNARE overproduction usually alleviates defects in partner SNAREs (Couve and Gerst, 1994; Fischer von Mollard *et al*., 1997; Pelham, 1997), this appeared to preclude their participation in SV fusion.

Despite the lack of effect, Sso was able to precipitate (in descending order of amount) with tagged Vti1, Nyv1, Tlg1, Bos1 and Tlg2 from untreated *snc* cells (Figure 4C). However, upon treatment with C_2-ceramide, all were unable to precipitate Sso, with the exception of Snc1, which served as a positive control (Figure 4C). About 8% of Sso co-immunoprecipitated with the tagged Snc1, in both treated and untreated cells. Thus, non-specific Sso–SNARE interactions are evident in untreated cells but confer no enhancement of growth, and are eliminated upon ceramide treatment and subsequent Sso dephosphorylation.

Tagged and native Sso–t-SNAREs co-precipitate

Since no other SNARE appears to contribute a functional helix to the exocytic complex, we postulated that Sso proteins assemble *in trans* to form a functional SNARE complex with Sec9. To verify that Sso proteins can associate and perhaps form a 2:1 Sso–Sec9 SNARE complex, we immunoprecipitated HA-tagged Sso1 (12.6% of total) from *snc* cell lysates with anti-HA abs and probed for the presence of untagged Sso in the precipitates (Figure 4D). We found that untagged Sso (12% of total) co-immuno-precipitated with HA-Sso1 at a ratio of 1:1.9, as determined by quantitative western analysis (Figure 4D and E). Since HA-Sso1 was expressed at a level 2-fold higher than that of Sso (Figure 4D and E), the ratio of untagged to tagged proteins averages 1:1 within the immunoprecipitated complex, after normalization for expression. While this does not exclude the possibility of Sso multimerization, it does suggest that Sso proteins can form dimers.

Mutation of Ser79 in Sso1 rescues snc cells in the absence of ceramide

As SNARE assembly and exocytosis correlates with dephosphorylation, we examined potential sites for phosphorylation in Sso1. Sso1 possesses two PKA (e.g. Thr66 and Ser79), two PKC (e.g. Thr109 and Ser255) and numerous casein kinase II phosphorylation sites. The two PKA sites looked interesting, as they localize to a putative auto-inhibitory domain of Sso (Nicholson *et al*., 1998). Moreover, overexpression of an activator of the PKA pathway, *RAS1*, inhibited the growth of *snc* yeast (not shown). In contrast, overexpression of an activated allele
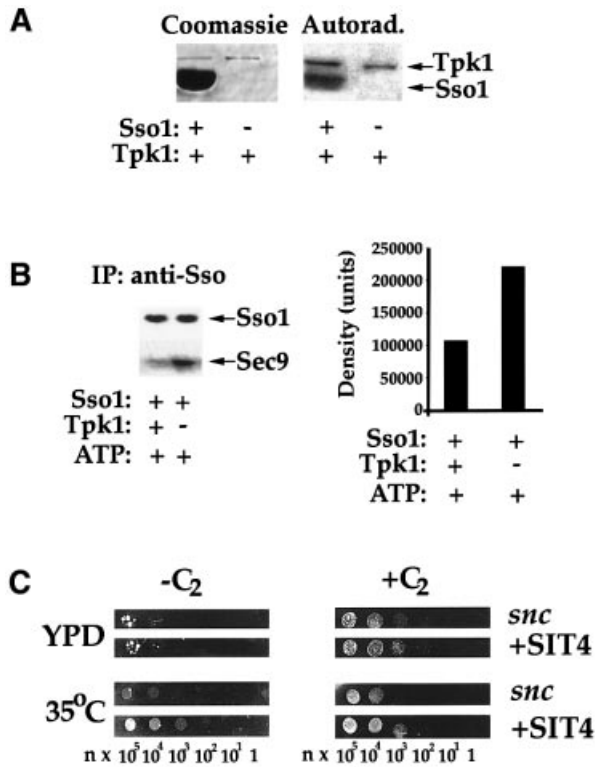
Fig. 6. Phosphorylation of Sso *in vitro* by Tpk1 inhibits SNARE assembly. (**A**) Sso1[1–265] is phosphorylated *in vitro* by Tpk1. Purified GST–Sso1 was incubated with or without recombinant Tpk1 in the presence of [γ-^{32}P]ATP. Samples were resolved by SDS–PAGE and detected by Coomassie Blue staining or autoradiography. (**B**) Phosphorylated Sso1[1–265] is deficient in its ability to form complexes with Sec9[402–651]. *In vitro* phosphorylated and non-phosphorylated GST–Sso1[1–265] were incubated with GST–Sec9[402–651], after which samples were immunoprecipitated, resolved by SDS–PAGE and quantified by antibody detection. (**C**) *SIT4* overexpression partially rescues *snc* cells. *snc* null cells transformed with a plasmid expressing Sit4 (+SIT4), or a control plasmid (*snc*), were grown and plated onto SC (35°C) and rich medium (YPD) with (+C$_2$) or without (–C$_2$) added C$_2$-ceramide. Cells were grown for 36 h.

of *PKC1* (*PKC1-R398P*) (Philips and Herskowitz, 1997) had no effect.

Substitution of Ser79 with alanine in Sso1 (*SSO1*[Ala79]) and its overexpression greatly enhanced the growth of *snc* cells at 26°C and resulted in their full rescue on YPD (Figure 5A), even in the absence of ceramide. In contrast, the substitution of Thr66 with alanine could not enhance growth, and overexpression of native Sso had only a mild effect. Thus, abolishment of a single putative PKA site (Ser79) in Sso1 was sufficient to restore near-normal growth. Interestingly, deletion mutants (e.g. *SSO1*[Δ1–103] and *SSO1*[Δ1–146]) that lack the putative N-terminal auto-inhibitory domain (and both PKA sites) and expressed well in yeast did not enhance growth. This indicates an essential role for this domain *in vivo*.

Phosphorylation of Sso1[Ala79] was determined by meta-bolic labeling (Figure 5B). Sso1[Ala79] phosphorylation was almost undetectable in untreated *snc* cells, and was comparable to that of native Sso after ceramide treatment (Figure 5B). Analysis of the complex formed between Sso1[Ala79] and Sec9 (as assayed by co-IP) showed that

similar amounts were formed under all conditions (Figure 5C). We found that 6.9 and 9.1% (0.66 E-7 and 0.78 E-7 mol) of Sso1[Ala79] precipitated with anti-Sec9 abs before and after treatment, respectively. In contrast, only 2.7% of native Sso1 complexed with Sec9 in the absence of ceramide, while 6.5% precipitated in its presence (0.22 E-7 and 0.55 E-7 mol, respectively). Thus, Sso1[Ala79] is a hypo-phosphorylated form of Sso1 that forms productive SNARE complexes in the absence of ceramide. This lends credence to the idea that dephosphorylation and complex formation are coupled.

Phosphorylation of Sso1 by Tpk1 in vitro reduces its ability to form SNARE complexes

The experiments above demonstrate that phosphoryl-ation of Sso reduces its ability to form SNARE complexes *in vivo*. To verify this using an alternative strategy, we used recombinant glutathione *S*-transferase (GST)–Sso1[1–265] and phosphorylated it *in vitro* using recombinant GST–Tpk1. We found that ~1.5 mol of phosphate were incorporated per mol y of Sso1 under the reaction conditions used (1.3 E-7 mol of phosphate incorporated into 8.9 E-8 mol of Sso1) (Figure 6A), indicating the presence of 1–2 usable Tpk1 sites per molecule. Next, in binding assays performed with recombinant Sec9, we found that phosphorylated GST–Sso1[1–265] was less able (by 2-fold) to assemble into SNARE complexes (Figure 6B). IP of this SNARE complex with anti-Sso abs revealed a Sso:Sec9 ratio of 1.96:1 in the precipitates, in the absence of Tpk1.

Over-production of the catalytic subunit of CAPP partially rescues snc cells

As ceramide treatment induces Sso dephosphorylation and SNARE assembly, we examined whether overexpression of the catalytic subunit of CAPP, Sit4 (Nickels and Broach, 1996), could rescue *snc* cells by itself (Figure 6). We found that *SIT4* overexpression improved growth at 35°C, suggesting that it mediates the effect of ceramide in part. Addition of C$_2$-ceramide to *SIT4* overexpressing cells gave an effect stronger than ceramide addition or *SIT4* overexpression alone. This suggests either that Sit4 may not be fully active without overexpression of its regulatory subunits or, perhaps, that another phosphatase is involved.

To address the latter, we overexpressed phosphatases bearing domains conserved in Sit4, including Pph21 and Pph3, which also complex with the regulatory subunits of CAPP (Jiang and Broach, 1999). However, only Sit4 and neither Pph21 nor Pph3 rescued *snc* yeast (not shown).

Discussion

The idea that protein phosphorylation modulates exo-cytosis stems from the use of inhibitors and activators of protein kinases and phosphatases, which showed an impact upon stimulus-coupled secretion (i.e. neuronal transmission) and synaptic vesicle recycling (Greengard *et al.*, 1993; Gerst, 1999; Turner *et al.*, 1999). While important for illustrating the involvement of signaling cascades in protein trafficking and secretion, few of these works defined a clear and precise series of targets that might reveal the underpinnings of a
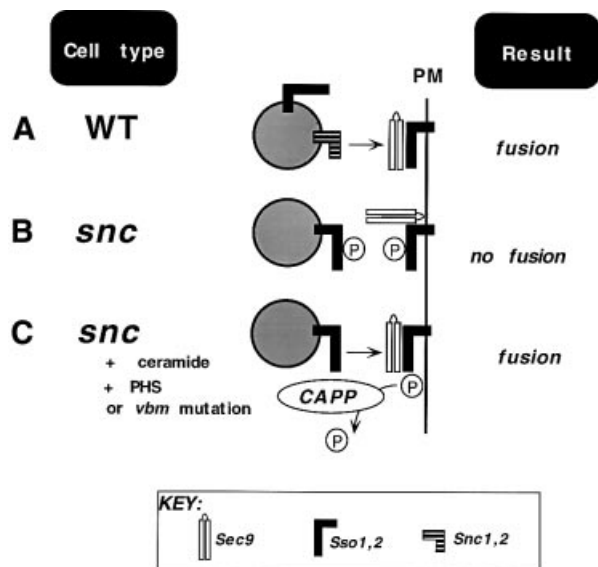
Fig. 7. A model for t-SNARE-mediated exocytosis. (**A**) In WT cells, v-SNAREs (Snc1,2) on the vesicle assemble into a functional SNARE complex with the partner t-SNAREs, Sso1,2 and Sec9, on the plasma membrane (PM). (**B**) *snc* cells, which lack the exocytic v-SNAREs, are unable to confer vesicle docking and fusion due to hyper-phosphorylation (P) of the Sso t-SNAREs. (**C**) *snc* cells treated with C_2-ceramide or PHS, or bearing an inactivating mutation in either *VBM* gene, activate the ceramide-activated protein phosphatase (CAPP). CAPP dephosphorylates Sso, allowing Sso to assemble *in trans* into a t–t-SNARE complex, restoring docking and fusion.

regulatory mechanism. Our understanding of SNAREs as pivotal mediators of membrane docking and fusion has thrust them into the spotlight as potential substrates for signaling cascades that impinge upon exocytic processes.

Studies performed both *in vivo* and *in vitro* reveal that SNAREs and SNARE regulatory proteins undergo phosphorylation by kinases. For example, *in vitro* phosphorylation of SNAP-25 by PKC, or phosphorylation of Munc-18 by cyclin-dependent kinase 5, results in a decrease in the affinity for syntaxin (Shimazaki *et al.*, 1996; Shuang *et al.*, 1998). Syntaxins are phosphorylated *in vitro* by a variety of kinases, resulting in a reduced affinity for their SNARE partners (Hirling and Scheller, 1996; Foster *et al.*, 1998), while increasing the affinity for synaptotagmin (Risinger and Bennett, 1999). Thus, a role for signal-induced protein kinases in SNARE complex assembly is likely. A recent study has even described a kinase that associates with a syntaxin and phosphorylates SNAP-23 (Cabaniols *et al.*, 1999). SNAP-23 phosphorylation was proposed to inhibit t-SNARE assembly *in vitro*; however, an opposite effect upon assembly was observed *in vivo*. Neither the mechanism controlling SNAP-23 phosphorylation nor the identity of the phosphorylated residues are known.

Here, we show that treatment with ceramide precursors and analogs allows yeast to overcome specific blocks in exocytosis. These blocks include cells lacking their full complement of exocytic v-SNAREs (*snc* null cells) or bearing a *ts* mutation in Sso2 (*sso2-1* cells), a syntaxin family member. Mechanistically, we have shown that rescue occurs via dephosphorylation of the Sso t-SNAREs (Figures 3 and 5) by a type 2A phosphatase activity

[composed of the *CDC55*, *TPD3* and *SIT4* gene products (Nickels and Broach, 1996)] (Figures 1 and 6). The decrease in Sso phosphorylation *in vivo* results in an enhanced ability to form SNARE complexes (Figures 4 and 5) and a heightened rate of protein trafficking and secretion (Figure 2). Thus, a sphingoid base/ceramide-induced signaling cascade overcomes constraints placed upon the t-SNAREs by kinases involved in cell growth and proliferation. This relief is likely to be part of a stress-response pathway controlled by ceramides and their precursors, of which there is evidence from both yeast and mammals (Hannun and Luberto, 2000). Interestingly, a role for sphingoid base synthesis in endocytosis (Zanolari *et al.*, 2000) has been described, although the mechanism is not fully known and does not involve Sit4 (Friant *et al.*, 2000).

Our work suggests that PKA is involved in the regulation of exocytosis, as the mutation of a single PKA phosphorylation site allows a mutant Sso1 (Sso1[Ala79]) to confer growth in the absence of ceramide (Figure 5). Moreover, phosphorylation of a recombinant form of Sso1 by Tpk1 *in vitro* inhibited assembly into complexes with recombinant Sec9 (Figure 6). Thus, growth control by the RAS–adenylyl cyclase–PKA signaling pathway includes modulation of intracellular protein trafficking and secretion. Why t-SNAREs are hyperphosphorylated in *snc* cells remains unclear; thus, more work is required to elucidate how the PKA signaling pathway modulates secretion. It is of interest, however, that the effects of this signaling pathway are balanced by the actions of Sit4 and the ceramide-activated stress response pathway. This explains why mutations in the *VBM/ELO* genes rescue cells that are secretion challenged (i.e. *snc* cells) and produce an effect identical to, if not more efficacious than the exogenous addition of active sphingoid bases or ceramides (Figure 3; David *et al.*, 1998). Our results also suggest that ceramides and SLs play distinct roles in protein transport and SV trafficking. Ceramides, being SL precursors and degradation products, modulate signaling cascades directly related to growth control. SLs are likely to play structural roles, in terms of mediating membrane rigidity, thickness and the formation of cholesterol-rich micro-domains (Simons and Ikonen, 1997).

Here, we have connected several intriguing phenomena that play important roles in modulating SV docking and fusion. First, we have shown that the phosphorylation state of t-SNAREs correlates strongly with SNARE complex assembly both *in vitro* and *in vivo*, thus defining a role for post-translational modification (by PKA) in the regulation of exocytosis. Secondly, we have shown that a ceramide-mediated signaling pathway, known for its involvement in cell cycle control, enhances exocytosis by dephosphorylating t-SNAREs (via the actions of the Sit4 phosphatase). Interestingly, an earlier study demonstrated a role for a type 1A phosphatase in conferring ER–Golgi and vacuolar membrane fusion steps (Peters *et al.*, 1999). While the site of action for this phosphatase is unknown, our work implies that SNAREs involved in those transport steps are likely targets. Finally, we provide further evidence showing that t-SNAREs alone are sufficient to confer specificity and function to the docking and fusion event, as proposed (David *et al.*, 1998). This is supported by studies that show

Table I. Strains used in this study

Name	Genotype	Source
SP1	*MAT**a** ura3 leu2 trp1 ade8 can1 his3*	M.Wigler
SF750-14Dα	*MATα ura3-52 leu2-3,112 his4-580 sec1-1*	R.Schekman
NY774	*MATα ura3-52 leu2-3,112 sec4-8*	P.Novick
NY778	*MATα ura3-52 leu2-3,112 sec6-4*	P.Novick
RSY979	*MATα ura3-52 sec7-5*	R.Schekman
NY782	*MAT**a** ura3-52 leu2-3,112 sec9-4*	P.Novick
NY1217	*MAT**a** ura3-52 leu2-3,112 sec18-1*	P.Novick
RSY1010	*MAT**a** ura3-52 sec21-1*	R.Schekman
RSY324	*MAT**a** ura3-52 sec22-2*	R.Schekman
H458	*MAT**a** ura3-52 leu2-3, 112 sso1::HIS3 sso2-1*	H.Ronne
JG8	*MAT**a** can1 leu2 trp1 snc1::URA3 snc2::ADE8 pTGAL-SNC1 or pLGAL-SNC1*	J.Gerst
DD1	*MAT**a** his3 leu2 snc1::URA3 snc2::ADE8 vbm1::TRP1 pLGAL-SNC1*	J.Gerst
SS1	*MAT**a** his3 leu2 snc1::URA3 snc2::ADE8 vbm2::LEU2 pTGAL-SNC1*	J.Gerst
DD3	*MAT**a** ura3 trp1 ade8 can1 his3 vbm1::LEU2*	J.Gerst
SS3	*MAT**a** ura3 trp1 ade8 can1 his3 vbm2::LEU2*	J.Gerst

Table II. Plasmids and vectors used in this study

Plasmid name	Gene expressed	Vector	Sites of cloning	Oligo name
pADH-HABOS1	*BOS1*	pAD54	*Sal*I and *Sac*I	BOS1-f, BOS1-r
pADH-mycNYV1	*NYV1*	pAD6	*Sal*I and *Sac*I	NYV1-f, NYV1-r
pADH-HATLG2	*TLG2*	pAD4Δ	*Sal*I and *Sac*I	TLG2-f, TLG2-r
pADH-HAPEP12	*PEP12*	pAD54	*Sal*I and *Sac*I	PEP12-f, PEP12-r
pADH-mycBET1	*BET1*	pAD6	*Sal*I and *Sac*I	BET1-f, BET1-r
pADH-mycSEC22	*SEC22*	pAD6	*Sal*I and *Sac*I	SEC22-f, SEC22-r
pADH-HAVTI1	*VTI1*	pAD4Δ	*Sal*I and *Sac*I	VTI1-f, VTI1-r
pADH-HASSO1	*SSO1*	pAD54	*Sal*I and *Sac*I	SSO1-f, SSO1-r
pALTER-SSO1	*SSO1*	pALTER	*Sal*I and *Sac*I	SSO1-f, SSO1-r
pADH-HATLG1[a]	*TLG1*	pAD4Δ	*Sal*I and *Sac*I	TLG1-f, TLG1-r
YEpSIT4	*SIT4*	YEp13M4	*Sal*1 and *Bam*HI	SIT4-f, SIT4-r
pGex-TPK1	*TPK1*	pGex-4T-3	*Eco*RI and *Xho*I	TPK1-f, TPK1-r
YEpPPH3	*PPH3*	YEp13M4	*Sal*I	PPH3-f, PPH3-r
YEpPPH21	*PPH21*	YEp13M4	*Sal*I	PPH21-f, PPH21-r
pALTER-SSO1-A66[b]	*SSO1(A66)*	pALTER	*Sal*I and *Sac*I	SSO1-A66
pALTER-SSO1-A79[b]	*SSO1(A79)*	pALTER	*Sal*I and *Sac*I	SSO1-A79
pADHmycSSO1-A66[c]	*SSO1(A66)*	pAD6	*Sal*I and *Sac*I	–
pADH-mycSSO1-A79[c]	*SSO1(A79)*	pAD54	*Sal*I and *Sac*I	–
PADH-mycSSO1Δ1-103	*SSO1(Δ1–103)*	pAD6	*Sal*I and *Sac*I	SSO1Δ1–103-f, SSO1-r
PADH-mycSSO1ΔA1-146	*SSO1(Δ1–146)*	pAD6	*Sal*I and *Sac*I	SSO1Δ1–146-f, SSO1-r

Oligonucleotide sequences will be provided upon request.
[a]This plasmid was created by D.Chapman-Shimshoni.
[b]This plasmid was created to allow the site-directed mutagenesis of *SSO1*.
[c]Mutagenized alleles of *SSO1* were transfered from pALTER into either pAD6 or pAD54.

a sole requirement for t-SNAREs in the fusion of ER membranes (Patel *et al.*, 1998) and vacuoles in yeast (Nichols *et al.*, 1997). Moreover, other works have shown that syntaxins associate, being shown to bind SNAP-25 at a 2:1 ratio (Fasshauer *et al.*, 1997) and to undergo dimerization (Banfield *et al.*, 1994). In the analysis of our work, we noticed that the molar equivalents of Sso and Sec9 in the precipitated complexes were always close to a 2:1 molar ratio, whether from ceramide-treated or untreated cells (see Figures 4B and E, and 5C). While an imperfect measure of stoichiometry, it lends credence to the idea that a 2:1 Sso–Sec9 Q-SNARE fusion complex can form (F.M.Hughson, personal communication). More work will be required to substantiate this, but as Sso is present on secretory vesicles (David *et al.*, 1998; Lustgarten and Gerst, 1999) the possibility must be strongly considered. Notably, a recent study suggested that other v-SNAREs (e.g. Nyv1 and Sec22) can partner with Sso and Sec9 to confer fusion *in vitro* (McNew *et al.*, 2000). However, these SNARE interactions were measured out of context from those in living cells, wherein phosphorylation and other forms of SNARE regulation are likely to take place. Thus, based upon our work it seems likely that Sso proteins arrayed *in trans* (between vesicle and PM) form productive SNARE complexes with Sec9, and lead to membrane fusion in *snc* yeast (see model, Figure 7), the caveat being that the Sso t-SNAREs must be dephosphorylated so that assembly can proceed.

Materials and methods

Media and growth tests

Yeast were grown on standard media (Rose, 1990). C_2-ceramide, dihydro-C_2-ceramide, sphinganine (Calbiochem) and PHS (Sigma)

were dissolved in ethanol (at 15 mM or 1 mg/ml) and added to media to yield a final concentration of 10 µM for all reagents, except for PHS, for which 25 µM was used. For growth tests, yeast were counted using a hemocytometer, diluted serially, and plated by drops onto solid medium pre-incubated at different temperatures containing the various reagents. For batch treatment, cells were cultured overnight in medium containing the sphingoid base or ceramide analog.

Yeast strains
Yeast strains are listed in Table I.

Plasmids
Vectors included: YEp13M4 (2µ, *LEU2*); pTV3 (2µ, *TRP1*); pAD4Δ (2µ, *LEU2*, *ADH1* promoter); and pAD54 and pAD6, the same as pAD4Δ but containing sequences encoding the HA or Myc epitopes, respectively. Expression plasmids for *SNC1* and *SNC2* included: pADH-SNC1 (Gerst *et al.*, 1992), pTGAL-SNC1 and pADH-HASNC1 (Protopopov *et al.*, 1993), and pAHGAL-SNC2 (David *et al.*, 1998). Expression plasmids for the *SSO* genes included: pB100 (*ADH-SSO1*) and pB103 (*ADH-SSO2*) (Aalto *et al.*, 1993). pGEX plasmids for the bacterial expression of GST gene fusions with Sso[1–265] or Sec9[402–651] were provided by P.Brennwald. Plasmids created for this study are shown in Table II. Sequences of the oligonucleotides used will be provided upon request.

Metabolic labeling studies
Metabolic labeling of sphingolipids. Metabolic labeling of SLs using [³H]*myo*-inositol was as described (David *et al.*, 1998).

Protein phosphorylation. Yeast were grown to log phase in synthetic medium, switched to medium lacking phosphate for 3 h, and then pulsed for 2–3 h with [³²P]orthophosphate (50 µCi/OD$_{600}$ unit, 5 OD$_{600}$ units per sample). Following labeling, cells were washed and lysed using glass beads, in a phosphate-buffered solution containing 1% SDS, 150 mM NaCl, 10 mM sodium phosphate pH 7.0, 10 µg/ml soybean trypsin inhibitor, 10 µg/ml leupeptin, 10 µg/ml aprotinin, 100 µM MG132, 0.5 mM vanadate and 50 mM orthophosphate. Labeled proteins were immunoprecipitated from extracts as described (Couve *et al.*, 1995). Precipitates were resolved by SDS–PAGE, following which the gels were fixed, dried and exposed for radiography.

Phosphorylation of Sso[1–265] was performed at 30°C for 45 min using 5 µg of purified GST–Sso[1–265] mixed with 0.5 µg of purified GST–Tpk1, 50 µCi of [γ-³²P]ATP (5 Ci/µmol) and in a buffer containing 100 mM Tris–HCl pH 6.8, 20 mM magnesium acetate, 100 mM NaCl, and between 10 µM and 1 mM of unlabeled ATP. Samples were resolved by SDS–PAGE and exposed for autoradiography; in parallel, dilutions of [γ-³²P]ATP (1–6 µl of 1 E-10 Ci) were blotted and autoradiographed to yield a standard curve for measuring incorporation.

Pulse–chase analysis. Intracellular protein processing was monitored by pulse–chase analysis using [³⁵S]methionine (Amersham), as described (Couve *et al.*, 1995). Anti-Gas1 abs were a gift of H.Riezman.

Measurement of SNARE complexes
IP from lysates. SNARE complexes present in cell lysates were monitored by co-IP (Couve and Gerst, 1994). The following additions to the lysis and IP buffers were made, including 1% NP-40 (instead of Triton X-100), MG132 (100 µM), ATPγS (20 µM), EDTA (2 mM) and *N*-ethylmaleimide (1 mM), to inhibit SNARE complex dissociation and degradation. Affinity-purified anti-Sso and anti-Sec9 abs, along with anti-myc (gifts of P.Brennwald) and anti-HA (gift of M.Wigler) abs, were used for IP (1 µl per reaction) and detection. In these experiments, 10–14% of total Sso protein was immunoprecipitated using the anti-Sso abs, while 12–13% of HA-tagged Sso proteins were immunoprecipitated using anti-HA abs. The amount of Sec9 that immunoprecipitated with anti-Sec9 abs varied from 12 to 20%. Samples of TCLs, immunoprecipitates and resulting supernatants were resolved by SDS–PAGE and detected by western analysis to determine the amount of Sec9 or Sso that either immunoprecipitated or co-immunoprecipitated with a given antiserum. Quantitative detection was performed using [¹²⁵I]protein A (1 µCi/blot) and visualized by phosphoimager. Molar quantification of the SNAREs was determined using known amounts of GST–t-SNARE fusion proteins (Sso1[1–265] and Sec9[402–651]) that were purified over glutathione–Sepharose beads (Pharmacia), electrophoresed and detected in parallel to the IP reactions.

SNARE assembly in vitro. Recombinant affinity-purified GST–Sso1[1–265] (*in vitro* phosphorylated or non-phosphorylated) and GST–Sec9[402–651]

proteins were mixed together at a ratio of 1:1 (5 µg each) in buffer containing 0.5%NP-40 in phosphate-buffered saline, and allowed to incubate overnight at 4°C. Following which, proteins were immunoprecipitated with anti-Sso abs, resuspended in sample buffer and resolved by SDS–PAGE. Detection and quantification of the proteins using anti-Sec9 and -Sso abs were as described above.

Invertase assay
Invertase secretion was measured as described (Goldstein and Lampen, 1975). Secreted and non-secreted activities were determined from glucose-repressed and de-repressed cells, and measured in units based upon absorption at 540 nm (1 unit = 1 µmol glucose released/min/100 mg dry cells).

References

Aalto,M.K., Ronne,H. and Keranen,S. (1993) Yeast syntaxins Sso1p and Sso2p belong to a family of related membrane proteins that function in vesicular transport. *EMBO J.*, **12**, 4095–4104.

Banfield,D.K., Lewis,M.J., Rabouille,C., Warren,G. and Pelham,H.R. (1994) Localization of Sed5, a putative vesicle targeting molecule, to the *cis*-Golgi network involves both its transmembrane and cytoplasmic domains. *J. Cell Biol.*, **127**, 357–371.

Cabaniols,J.-P., Ravichandran,V. and Roche,P.A. (1999) Phosphorylation of SNAP-23 by the novel kinase SNAK regulates t-SNARE complex assembly. *Mol. Biol. Cell*, **10**, 4033–4041.

Carr,C.M., Grote,E., Munson,M., Hughson,F.M. and Novick,P.J. (1999) Sec1p binds to SNARE complexes and concentrates at sites of secretion. *J. Cell Biol.*, **146**, 333–344.

Couve,A. and Gerst,J.E. (1994) Yeast Snc proteins complex with Sec9. Functional interactions between putative SNARE proteins. *J. Biol. Chem.*, **269**, 23391–23394.

Couve,A., Protopopov,V. and Gerst,J.E. (1995) Yeast synaptobrevin homologs are modified posttranslationally by the addition of palmitate. *Proc. Natl Acad. Sci. USA*, **92**, 5987–5991.

David,D., Sundarababu,S. and Gerst,J.E. (1998) Involvement of long chain fatty acid elongation in the trafficking of secretory vesicles in yeast. *J. Cell Biol.*, **143**, 1167–1182.

Fasshauer,D., Otto,H., Eliason,W.K., Jahn,R. and Brunger,A.T. (1997) Structural changes are associated with soluble *N*-ethylmaleimide-sensitive fusion protein attachment protein receptor complex formation. *J. Biol. Chem.*, **272**, 28036–28041.

Fasshauer,D., Sutton,R.B., Brunger,A.T. and Jahn,R. (1998) Conserved structural features of the synaptic fusion complex: SNARE proteins reclassified as Q- and R-SNAREs. *Proc. Natl Acad. Sci. USA*, **95**, 15781–15786.

Ferro-Novick,S. and Jahn,R. (1994) Vesicle fusion from yeast to man. *Nature*, **370**, 191–193.

Fischer von Mollard,G., Nothwehr,S.F. and Stevens,T.H. (1997) The yeast v-SNARE Vti1p mediates two vesicle transport pathways through interactions with the t-SNAREs Sed5p and Pep12p. *J. Cell Biol.*, **137**, 1511–1524.

Fishbein,J.D., Dobrowsky,R.T., Bielawska,A., Garrett,S. and Hannun,Y.A. (1993) Ceramide-mediated growth inhibition and CAPP are modified in *S. cerevisiae*. *J. Biol. Chem.*, **268**, 9255–9261.

Foster,L.J., Yeung,B., Mohtashami,M., Ross,K., Trimble,W.S. and Klip,A. (1998) Binary interactions of the SNARE proteins syntaxin-4, SNAP23 and VAMP-2 and their regulation by phosphorylation. *Biochemistry*, **37**, 11089–11096.

Friant,S., Zanolari,B. and Riezman,H. (2000) Increased protein kinase or decreased PP2A activity bypasses sphingoid base requirement in endocytosis. *EMBO J.*, **19**, 2834–2844.

Gerst,J.E. (1997) Conserved α-helical segments on yeast homologs of the synaptobrevin/VAMP family of v-SNAREs mediate exocytic function. *J. Biol. Chem.*, **272**, 16591–16598.

Gerst,J.E. (1999) SNAREs and SNARE regulators in membrane fusion and exocytosis. *Cell. Mol. Life Sci.*, **55**, 707–734.

Gerst,J.E., Rodgers,L., Riggs,M. and Wigler,M. (1992) *SNC1*, a yeast homolog of the synaptic vesicle-associated membrane protein/synaptobrevin gene family: genetic interactions with the *RAS* and *CAP* genes. *Proc. Natl Acad. Sci. USA*, **89**, 4338–4342.

Goldstein,A. and Lampen,J.O. (1975) β-D-fructofuranoside fructo-hydrolase from yeast. *Methods Enzymol.*, **42**, 504–511.

Gotte,M. and Fischer von Mollard,G. (1998) A new beat for the SNARE drum. *Trends Cell Biol.*, **8**, 215–218.

Greengard,P., Valtorta,F., Czernik,A.J. and Benfenati,F. (1993) Synaptic vesicle phosphoproteins and regulation of synaptic function. *Science*, **259**, 780–785.

Gurunathan,S., Chapman-Shimshoni,D., Trajkovic,S. and Gerst,J.E. (2000) Yeast exocytic v-SNAREs confer endocytosis. *Mol. Biol. Cell*, **11**, 3629–3643.

Hannun,Y.A. and Luberto,C. (2000) Ceramide in the eukaryotic stress response. *Trends Cell Biol.*, **10**, 73–80.

Hirling,H. and Scheller,R.H. (1996) Phosphorylation of synaptic vesicle proteins: modulation of the α-SNAP interaction with the core complex. *Proc. Natl Acad. Sci. USA*, **93**, 11945–11949.

Jiang,Y. and Broach,J.R. (1999) Tor proteins and protein phosphatase 2A reciprocally regulate Tap42 in controlling cell growth in yeast. *EMBO J.*, **18**, 2782–2792.

Lester,R.L. and Dickson,R.C. (1993) Sphingolipids with inositolphosphate-containing head groups. *Adv. Lipid Res.*, **26**, 253–274.

Lustgarten,V. and Gerst,J.E. (1999) Yeast *VSM1* encodes a v-SNARE binding protein that may act as a negative regulator of constitutive exocytosis. *Mol. Cell. Biol.*, **19**, 4480–4494.

McNew,J.A., Parlati,F., Fukuda,R., Johnston,R.J., Paz,K., Paumet,F., Sollner,T.H. and Rothman,J.E. (2000) Compartmental specificity of cellular membrane fusion encoded in SNARE proteins. *Nature*, **407**, 153–159.

Nichols,B.J., Ungermann,C., Pelham,H.R., Wickner,W.T. and Haas,A. (1997) Homotypic vacuolar fusion mediated by t- and v-SNAREs. *Nature*, **387**, 199–202.

Nicholson,K.L., Munson,M., Miller,R.B., Filip,T.J., Fairman,R. and Hughson,F.M. (1998) Regulation of SNARE complex assembly by an N-terminal domain of the t-SNARE Sso1p. *Nature Struct. Biol.*, **5**, 793–802.

Nickels,J.T. and Broach,J.R. (1996) A ceramide-activated protein phosphatase mediates ceramide-induced G_1 arrest of *Saccharomyces cerevisiae*. *Genes Dev.*, **10**, 382–394.

Oh,C.-S., Toke,D.A., Mandala,S. and Martin,C.E. (1997) ELO2 and ELO3, homologues of the *Saccharomyces cerevisiae ELO1* gene, function in fatty acid elongation and are required for sphingolipid formation. *J. Biol. Chem.*, **272**, 17376–17384.

Patel,S.K., Indig,F.E., Olivieri,N., Levine,N.D. and Latterich,M. (1998) Organelle membrane fusion: a novel function for the syntaxin homolog Ufe1p in ER membrane fusion. *Cell*, **92**, 611–620.

Pelham,H.R. (1997) SNAREs and the organization of the secretory pathway. *Eur. J. Cell Biol.*, **74**, 311–314.

Peters,C., Andrews,P.D., Stark,M.J.R., Cesaro-Tadic,S., Glatz,A., Podtelejnikov,A., Mann,M. and Mayer,A. (1999) Control of the terminal step of intracellular membrane fusion by protein phosphatase I. *Science*, **285**, 1084–1087.

Philips,J. and Herskowitz,I. (1997) Osmotic balance regulates cell fusion during mating in *Saccharomyces cerevisiae*. *J. Cell Biol.*, **138**, 961–974.

Protopopov,V., Govindan,B., Novick,P. and Gerst,J.E. (1993) Homologs of the synaptobrevin/VAMP family of synaptic vesicle proteins function on the late secretory pathway in *S. cerevisiae*. *Cell*, **74**, 855–861.

Risinger,C. and Bennett,M.K. (1999) Differential phosphorylation of syntaxin and synaptosome-associated protein of 25 kDa (SNAP-25) isoforms. *J. Neurochem.*, **72**, 614–624.

Rose,M.D., Winston,F. and Hieter,P. (1990) *Methods in Yeast Genetics*. Cold Spring Harbor Laboratory Press, Cold Spring Harbor, NY.

Rothman,J.E. and Warren,G. (1994) Implications of the SNARE hypothesis for intracellular membrane topology and dynamics. *Curr. Biol.*, **4**, 220–233.

Shimazaki,Y., Nishiki,T., Omori,A., Sekiguchi,M., Kamata,Y., Kozaki,S. and Takahashi,M. (1996) Phosphorylation of 25-kDa synaptosome-associated protein. Possible involvement in protein kinase C-mediated regulation of neurotransmitter release. *J. Biol. Chem.*, **271**, 14548–14553.

Shuang,R., Zhang,L., Fletcher,A., Groblewski,G.E., Pevsner,J. and Stuenkel,E.L. (1998) Regulation of Munc-18/syntaxin 1A interaction by cyclin-dependent kinase 5 in nerve endings. *J. Biol. Chem.*, **273**, 4957–4966.

Simons,K. and Ikonen,E. (1997). Functional rafts in cell membranes. *Nature*, **387**, 569–572.

Sutton,R.B., Fasshauer,D., Jahn,R. and Brunger,A.T. (1998) Crystal structure of a SNARE complex involved in synaptic exocytosis at 2.4 Å resolution. *Nature*, **395**, 347–353.

Turner,K.M., Burgoyne,R.D. and Morgan,A. (1999) Protein phosphorylation and the regulation of synaptic membrane traffic. *Trends Neurosci.*, **22**, 459–464.

Weber,T., Zemelman,B.V., McNew,J.A., Westermann,B., Gmachl,M., Parlati,F., Sollner,T.H. and Rothman J.E. (1998) SNAREpins: minimal machinery for membrane fusion. *Cell*, **92**, 759–772.

Zanolari,B., Friant,S., Funato,K., Sutterlin,C., Stevenson,B.J. and Riezman,H. (2000) Sphingoid base synthesis requirement for endocytosis in *Saccharomyces cerevisiae*. *EMBO J.*, **19**, 2824–2833.